POLITECNICO DI TORINO
Repository ISTITUZIONALE

Using inerter-based dampers as vibrating barriers for non-invasive seismic protection of buildings

Original
Using inerter-based dampers as vibrating barriers for non-invasive seismic protection of buildings / Deastra, P., Domaneschi, M.. - In: PROCEDIA STRUCTURAL INTEGRITY. - ISSN 2452-3216. - 78:(2026), pp. 2038-2045. (20th ANIDIS Conference, 2025 Assisi (Ita) 7 settembre 2025 – 11 settembre 2025) [10.1016/j.prostr.2025.12.259].

Availability:
This version is available at: 11583/3010912 since: 2026-05-16T17:03:46Z

Publisher:
Elsevier

Published
DOI:10.1016/j.prostr.2025.12.259

Terms of use:

This article is made available under terms and conditions as specified in the corresponding bibliographic description in the repository

Publisher copyright

(Article begins on next page)

26 November 2026

Available online at www.sciencedirect.com

ScienceDirect

Procedia Structural Integrity 78 (2026) 2038–2045

Structural Integrity Procedia

www.elsevier.com/locate/procedia

XX ANIDIS Conference

Using inerter-based dampers as vibrating barriers for non-invasive seismic protection of buildings

Predaricka Deastra[a,*], Marco Domaneschi[a]

[a]*Department of Structural, Geotechnical and Building Engineering (DISEG), Politecnico di Torino, Turin, 10129, Italy*

Abstract

Inerter based dampers have shown great promise in structural vibration control, particularly for enhancing the seismic resilience of buildings. Among various implementation strategies, their use as vibrating barriers (ViBa) stands out due to the unique advantage of providing external and non-invasive vibration mitigation. When installed adjacent to the primary structure, an inerter based vibrating barrier (IViBa) engages through soil structure interaction, enabling effective energy dissipation without interfering with the structural integrity or architectural design of the main building. This makes the IViBa especially well suited for retrofitting existing buildings and for application in densely populated urban environments. In its conventional form, the IViBa has an inerter attached to its mass, forming a configuration known as a tuned mass damper inerter (TMDI). While effective, the IViBa with a TMDI configuration still requires a substantial physical mass to achieve satisfactory performance, which can limit its practicality. To address this challenge, this study explores the use of a tuned inerter damper (TID) configuration, where the inerter replaces the conventional IViBa mass entirely. The results demonstrate that the IViBa with a TID configuration can significantly reduce the required physical mass while maintaining the vibration mitigation performance of the system. Additionally, the internal motion of the IViBa is markedly reduced, resulting in lower stroke and reduced space demand, which further improves the feasibility, durability, and ease of implementation of the device in real world applications.

© 2025 The Authors. Published by ELSEVIER B.V.
This is an open access article under the CC BY-NC-ND license (https://creativecommons.org/licenses/by-nc-nd/4.0)
Peer-review under responsibility of XX ANIDIS Conference organizers

Keywords: vibration control; vibrating barriers (ViBa); soil-structure interaction; tuned mass damper inerter (TMDI); tuned inerter damper (TID).

1. Introduction

Recent advancements in earthquake protection technology have significantly enhanced the structural performance of buildings, enabling more effective energy dissipation and increased resilience against seismic events. One of the most promising developments is the incorporation of the inerter as an additional component in vibration control systems. Firslty introduced by Smith (2002), the inerter is a two-terminal device that generates force proportional to the relative acceleration between its terminals. The proportionality constant, known as inertance, is measured in

* Corresponding author. Tel.: +39 0110904835
E-mail address: predaricka.deastra@polito.it

2452-3216 © 2025 The Authors. Published by ELSEVIER B.V.
This is an open access article under the CC BY-NC-ND license (https://creativecommons.org/licenses/by-nc-nd/4.0)
Peer-review under responsibility of XX ANIDIS Conference organizers
10.1016/j.prostr.2025.12.259

kilograms. Depending on the mechanism, an inerter can achieve an inertance several hundred times greater than its physical mass. For instance, a mechanical geared inerter developed at the University of Cambridge can produce an inertance of 700 kg while having a physical mass of only 3.5kg (Papageorgiou et al. (2009)). This excellent feature of the inerter has attracted significant attention in the earthquake engineering community, motivating its integration into vibration control systems to improve seismic performance of buildings.

Several mechanisms for the physical realisation of inerters have been reported in the literature, including fluid-based inerters (De Domenico et al. (2019)), mechanical geared inerters (Papageorgiou et al. (2009)), flywheel inerters (Deastra et al. (2023)), and ball-screw inerters (Ikago et al. (2012)). A comprehensive review of inerter realisation methods is provided in Wagg (2021).

A notable example of the integration of inerter technology into vibration control systems is the inerter-based vibrating barrier (IViBa). The IViBa is the enhanced version of the conventional vibrating barrier (ViBa) with an additional inerter. The concept of ViBa was first introduced by Cacciola and Tombari (2015), featuring a parallel spring-dashpot mechanism coupled with an oscillating mass. It stands out for its distinctive role as an external, non-intrusive system for reducing structural vibrations. Positioned next to the main structure, as shown in Fig. 1(a), it leverages structure-soil–structure interaction (SSSI) to dissipate seismic energy efficiently, all while preserving the building's structural and architectural integrity. This makes the ViBa highly advantageous for upgrading existing buildings and use in densely populated urban environments.

As reported in Cacciola et al. (2020), the IViBa extends the conventional ViBa by adding an inerter connected to the oscillating mass, forming a configuration known as a tuned mass damper inerter (TMDI) Marian and Giaralis (2014), as shown in Fig. 1(b). The addition of the inerter enables the system to achieve a higher effective mass ratio without a corresponding increase in the physical mass. This feature substantially enhances the performance of vibration mitigation systems, especially in applications where weight and space constraints restrict the use of large secondary masses. Consequently, inerter-based configurations represent a highly promising solution for improving the effectiveness and practicality of the ViBa.

Despite the proven effectiveness of the current IViBa implementation based on the TMDI configuration, it continues to demand a considerable physical mass owing to the inclusion of the secondary mass. As shown in Cacciola et al. (2020), a minimum mass ratio of 0.25 was investigated to achieve effective vibration mitigation. This requirement can pose practical limitations, particularly in retrofitting scenarios or when available space is limited. To address this limitation, this study aims to investigate the performance of the IViBa in the absence of a secondary mass.

By eliminating the physical secondary mass, the system transitions from a tuned mass damper inerter (TMDI) to a tuned inerter damper (TID) configuration as illustrated in Fig. 1(c). The TID concept was first introduced by Lazar et al. (2014) as an alternative to the traditional tuned mass damper (TMD). The primary distinction between the TMDI and TID lies in the presence of the secondary mass, m_{IViBa}, which is also referred to in the literature as auxiliary mass (Deastra et al. (2025)). In this study, the TID is proposed as a novel configuration for the IViBa system, and its performance is evaluated in comparison to both the conventional ViBa and the IViBa with a TMDI configuration. This approach aims to preserve vibration mitigation effectiveness while significantly reducing the device's size, weight, and installation constraints, thereby enhancing its practicality for real-world applications.

The reminder of this paper is organized as follows: Section 2 discusses the analytical models and governing equations of the two IViBa configurations. Numerical optimisation and simulations in the frequency domain are presented in Sections 3 and 4, respectively. Conclusions are provided in Section 5.

2. Analytical models and governing equations for IViBa

The analytical model of a single-degree-of-freedom (SDOF) structure equipped with an IViBa, adapted from Cacciola et al. (2020), is illustrated in Fig. 1(a). The system consists of a lumped-mass SDOF structure characterized by mass m, stiffness k, and viscous damping coefficient c, supported on a compliant soil layer with mass m_f. The effects of soil–structure interaction (SSI) are captured using soil stiffness k_f and damping coefficient c_f. The structure is controlled by an IViBa device enclosed within a containment mass $m_{f,IViBa}$. The effects of structure-soil-structure interaction (SSSI) is represented by a spring and dashpot with stiffness k_{SSSI} and damping coefficient c_{SSSI}. Additionally, the SSI effects related to the IViBa containment are modeled using linear elements with stiffness $k_{f,IViBa}$ and

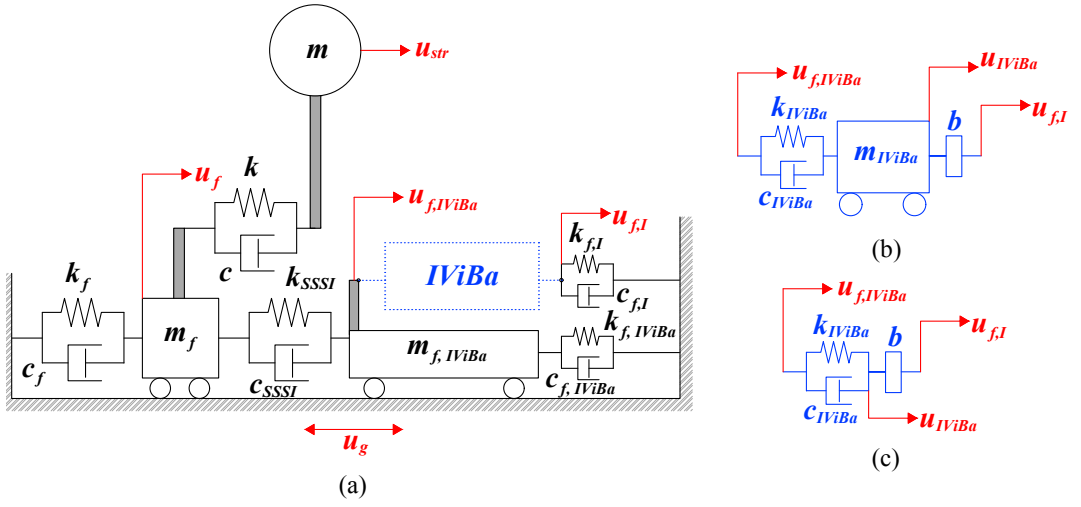


Fig. 1. (a) Analytical model of a single-degree-of-freedom structure equipped with an IViBa. (b) TMDI. (c) TID.

damping $c_{f,IViBa}$. The soil at the inerter's ground connection is represented by stiffness $k_{f,I}$ and damping coefficient $c_{f,I}$.

Two alternative IViBa configurations are illustrated in Fig. 1(b) and (c). The first configuration corresponds to the conventional ViBa, which consists of a spring and a dashpot arranged in parallel—with stiffness k_{IViBa} and damping coefficient c_{IViBa}—supporting a secondary mass m_{IViBa}. An inerter with inertance b is connected to the secondary mass, forming a TMDI configuration. The application of the TMDI as an IViBa was first investigated in Cacciola et al. (2020). The second configuration adopts the TID model, which can be regarded as a limiting case of the TMDI, where the secondary mass is negligible ($m_{IViBa} = 0$), offering a potentially more compact and lightweight alternative.

The equation of motion of the system shown in Fig. 1(a) in absolute coordinate can be written as

$$\mathbf{M}\ddot{\mathbf{u}}(t) + \mathbf{C}\dot{\mathbf{u}}(t) + \mathbf{K}\mathbf{u}(t) = \bar{\mathbf{C}}\dot{u}_g(t) + \bar{\mathbf{K}}u_g(t) \tag{1}$$

Considering the TMDI configuration, the $\mathbf{M}$, $\mathbf{C}$, $\mathbf{K}$, $\bar{\mathbf{C}}$ and $\bar{\mathbf{K}}$ matices are given as follows:

$$\mathbf{M} = \begin{bmatrix} m_f & 0 & 0 & 0 & 0 \\ 0 & m & 0 & 0 & 0 \\ 0 & 0 & m_{f,IViBa} & 0 & 0 \\ 0 & 0 & 0 & b + m_{IViBa} & -b \\ 0 & 0 & 0 & -b & b \end{bmatrix}; \mathbf{C} = \begin{bmatrix} c_f + c_{SSSI} + c & -c & -c_{SSSI} & 0 & 0 \\ -c & c & 0 & 0 & 0 \\ -c_{SSSI} & 0 & c_{SSSI} + c_{f,IViBa} + c_{IViBa} & -c_{IViBa} & 0 \\ 0 & 0 & -c_{IViBa} & c_{IViBa} & 0 \\ 0 & 0 & 0 & 0 & c_{f,I} \end{bmatrix}$$

$$\mathbf{K} = \begin{bmatrix} k_f + k_{SSSI} + k & -k & -k_{SSSI} & 0 & 0 \\ -k & k & 0 & 0 & 0 \\ -k_{SSSI} & 0 & k_{SSSI} + k_{f,IViBa} + k_{IViBa} & -k_{IViBa} & 0 \\ 0 & 0 & -k_{IViBa} & k_{IViBa} & 0 \\ 0 & 0 & 0 & 0 & k_{f,I} \end{bmatrix}; \bar{\mathbf{C}} = \begin{bmatrix} -c_f \\ 0 \\ -c_{f,IViBa} \\ 0 \\ -c_{f,I} \end{bmatrix}; \bar{\mathbf{K}} = \begin{bmatrix} -k_f \\ 0 \\ -k_{f,IViBa} \\ 0 \\ -k_{f,I} \end{bmatrix}$$

It should be noted that for the IViBa with a TID configuration, the IViBa mass m_{IViBa} should be set to zero. The transfer function of the system in the Laplace domain can be written as:

$$T(s) = \frac{\mathbf{U}(s)}{U_g(s)} = (\mathbf{M}s^2 + \mathbf{C}s + \mathbf{K})^{-1}(\bar{\mathbf{C}}s + \bar{\mathbf{K}}) \tag{2}$$

where s denotes the Laplace transform variable, defined as $s = i\omega$, with ω representing the angular frequency of the ground displacement input $u_g(t)$, and $i = \sqrt{-1}$. $\mathbf{U}(s)$ is the matrix of the displacement response in the Laplace domain, expressed as:

$$\mathbf{U}(s) = [U_f U_{str} U_{f,IViBa} U_{IViBa} U_{f,I}]^T \tag{3}$$

3. Numerical optimisation

To simulate optimum response of the single-degree-of-freedom (SDOF) structure, the IViBa parameters must be firstly optimised. In this study, a numerical optimisation method based on the Self-adaptive Differential Evolution (SaDE) algorithm proposed by Qin and Suganthan (2005) is utilized, with MATLAB used to implement the approach. SaDE is an enhanced version of the Differential Evolution (DE) algorithm (Storn and Price (1997)), designed to automatically select suitable learning strategies to effectively identify the global optimum of the specified objective function. For each generation, a set of candidate parameters is produced, and the total number of generations is determined by the point at which convergence is achieved. A comprehensive explanation of the SaDE algorithm is provided in Qin and Suganthan (2005).

The optimisation aims to minimise the magnitude of the ground-to-floor displacement transfer function, defined as:

$$\min\left(\max\left|\frac{U_{\text{str}}(s)}{U_g(s)}\right|\right). \tag{4}$$

This objective ensures that the structure experiences minimal displacement under harmonic excitation, thereby enhancing the effectiveness of the vibration mitigation system.

Figure 2 presents a comparison of the IViBa performance optimised using the H_2 optimisation approach in Cacciola et al. (2020) and that obtained using the SaDE algorithm in this paper. The optimal IViBa parameters corresponding to Fig. 2(a) and Fig. 2(b) are listed in Table 1 and Table 2, respectively. All other parameters are adopted from Cacciola and Tombari (2015) as given in Table 3. Accounting for the soil compliance and its foundation, the fundamental natural frequency of the SDOF structure is 22.62 rad/s (Cacciola et al. (2020)).

A comparison between Fig. 2(a) and Fig. 2(b) reveals that the lowest amplitude of the structural response around the natural frequency of 3.6 Hz is achieved using the H_2 optimisation approach in Cacciola et al. (2020), as shown in Fig. 2(a). However, this configuration also exhibits a higher maximum amplitude at other frequencies around resonance compared to the result in Fig. 2(b). In contrast, the SaDE-optimised configuration shown in Fig. 2(b) yields a more uniform response and effectively reduces the overall peak amplitude near the resonant frequency. This suggests that the optimisation procedure using the SaDE algorithm provides a better balance in suppressing the response at resonance and improving the robustness of the IViBa system across a wider frequency range.

Furthermore, Figs. 2(c) and 2(d) highlight significant differences between the two optimisation approaches in terms of the frequency response amplitude of the IViBa mass, u_{IViBa}. The optimisation method adopted in this study results in a notably lower amplitude of u_{IViBa}, which implies that the device experiences reduced internal motion. This can

lead to lower mechanical demands on the IViBa components, potentially improving durability and making the system more suitable for practical implementation.

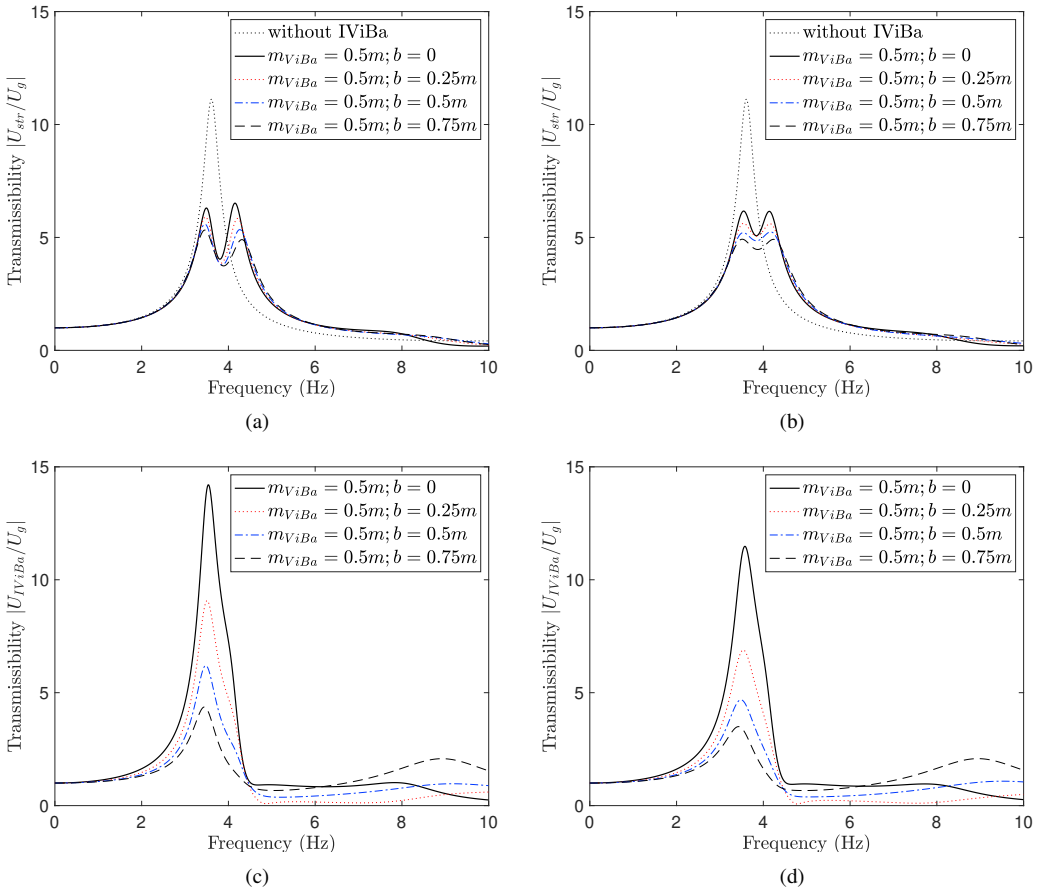


Fig. 2. Performance comparison of the IViBa with $m_{IViBa} = 0.5m$, optimized using two different approaches: (a) and (c) correspond to the method proposed in Cacciola et al. (2020), while (b) and (d) correspond to the method proposed in this study.

Table 1. Optimal parameters of the IViBa from Cacciola et al. (2020) used for the case in Fig. 2(a) and 2(c) for $m_{IViBa} = 0.5m$

Optimal parameters	$b = 0$	$b = 0.25$	$b = 0.5$	$b = 0.75$
k_{IViBa} (N/m)	195.52	360.61	667.38	1269.00
c_{IViBa} (Ns/m)	1.18	3.09	9.14	39.65

Table 2. Optimal parameters of the IViBa used for the case in Fig. 2(b) and 2(d) for $m_{IViBa} = 0.5m$

Optimal parameters	$b = 0$	$b = 0.25$	$b = 0.5$	$b = 0.75$
k_{IViBa} (N/m)	201.13	361.60	605.94	884.75
c_{IViBa} (Ns/m)	1.70	5.04	14.24	42.59

Table 3. Parameters for the model shown in Fig. 1(a) adopted from Cacciola and Tombari (2015)

Parameters	SDOF structure	SSI (structure)	SSI (IViBa)	SSSI	Inerter
Mass (kg)	$m = 0.59$	$m_f = 0.353$	$m_{f,IViBa} = 0.491$	-	$m_{f,I} = 0$
Stiffness (N/m)	$k = 909.85$	$k_f = 640$	$k_{f,IViBa} = 760$	$k_{SSSI} = 315$	$k_{f,I} = 760$
Damping coefficient (Ns/m)	$c = 4.0$	$c_f = 2.81$	$c_{f,IViBa} = 3.34$	$c_{SSSI} = 0.28$	$c_{f,I} = 3.34$

4. Frequency-domain simulations

The optimisation method using SaDE algorithm described in Section 3 is employed to determine the optimal values of k_{IViBa} and c_{IViBa} that minimise the amplitude of the structural response. An SDOF structure adopted from Cacciola et al. (2020) is used for simulation. The parameters of the structure, SSI and SSSI effects, as well as the soil compliance are given in Table 3. It should be noted that although the analytical model illustrated in Fig.1(a) represents a simplified version of a more complex real-world system, studies such as Cacciola and Tombari (2015) and Tombari et al. (2018) have demonstrated, through validation against advanced FEM/BEM simulations, that it delivers reliable accuracy for use in ViBa design applications.

Figure 3 compares the optimal performance between the IViBa with TID configuration and the conventional ViBa with the same mass ratios. The obtained optimal parameters are given in Table 4. As shown in Fig. 3(a), the conventioanl ViBa demonstrates slightly better performance in reducing the structural response, achieving approximately 2–5% greater reduction compared to the IViBa with TID configuration. When compared to the uncontrolled system, both control systems deliver substantial improvements—reducing the structural response by 33.11% with a mass ratio of 0.25, and by 50.37% with a mass ratio of 0.75. Interestingly, with the TID configuration, the motion amplitude of the secondary mass m_{IViBa} can be significantly reduced, as shown in Fig 3(b). This implies that the system is subject to lower mechanical demands and less required space for installation, hence increasing its practicality for real-world applications.

Next, comparison is made between the two IViBa configurations: TMDI ($m_{IViBa} > 0$) and TID ($m_{IViBa} = 0$). Figure 4(a) presents the frequency response of the SDOF structure for equivalent mass ratios of $1m$ and $0.75m$. The optimal parameters used for these configurations are listed in Table 5. As expected, the results show that a larger mass ratio leads to improved vibration mitigation performance. For a given mass ratio, the TMDI configuration provides slightly better performance compared to the TID configuration. This suggests that while the inerter significantly reduces the need for physical mass, its inclusion alone does not necessarily result in superior performance. Nonetheless, the difference in maximum response amplitudes between the two configurations is relatively small, approximately 1–2%.

Figure 4(b) shows the displacement response of the IViBa mass in the frequency domain. Similar to the previous case, the inclusion of the inerter significantly reduces the amplitude of the IViBa mass response, with the lowest displacement observed in the TID configuration ($m_{IViBa} = 0$). This implies that the TID configuration not only minimises structural response but also reduces internal motion within the device.

Table 4. Optimal parameters of the IViBa used for the case in Fig. 3

Optimal parameters	$m_{IViBa} = 0$; $b = 0.25m$	$m_{IViBa} = 0$; $b = 0.5m$	$m_{IViBa} = 0$; $b = 0.75m$	$b = 0$; $m_{IViBa} = 0.25m$	$b = 0$; $m_{IViBa} = 0.5m$	$b = 0$; $m_{IViBa} = 0.75m$
k_{IViBa} (N/m)	117.45	328.70	632.70	94.92	201.13	319.85
c_{IViBa} (Ns/m)	0.63	2.37	18.71	0.62	1.7	3.64

5. Conclusion

This study investigated the optimal performance of IViBa systems for seismic protection of structures, focusing on two configurations: TMDI (with auxiliary mass) and TID (without auxiliary mass). A numerical optimisation approach

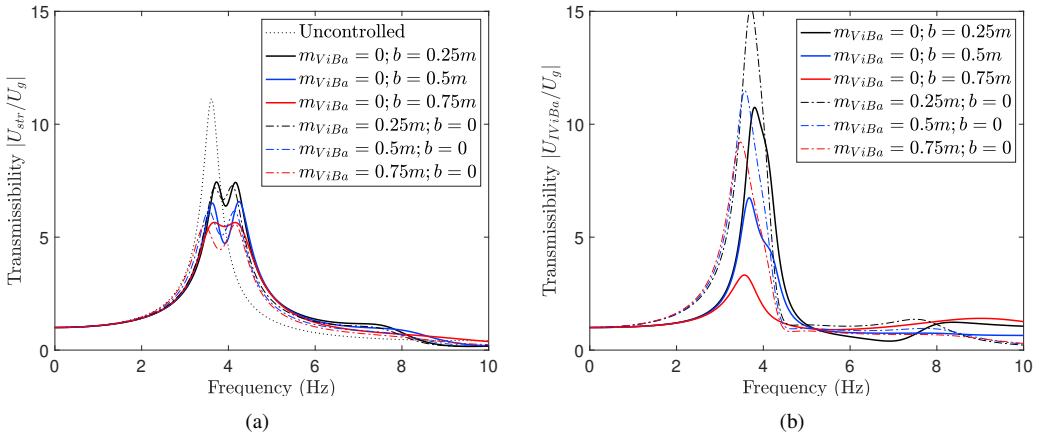


Fig. 3. Performance comparison between the conventioanl ViBa ($b = 0$) and the IViBa with TID configuration on the frequency response of the (a) SDOF structure, and (b) IViBa mass

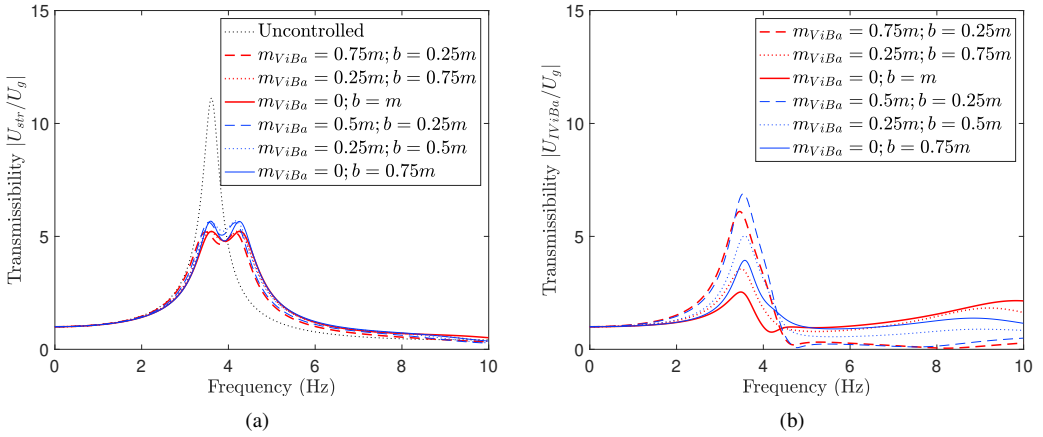


Fig. 4. Performance comparison of the two IViBa configurations on the frequency response of the (a) SDOF structure, and (b) IViBa mass. Here red and blue lines correspond to the equivalent mass ratio of 1 and 0.75, respectively.

Table 5. Optimal parameters of the IViBa used for the case in Fig. 4

Optimal parameters	$m_{IViBa} = 0.75m$; $b = 0.25m$	$m_{IViBa} = 0.25m$; $b = 0.75m$	$m_{IViBa} = 0$; $b = m$	$m_{IViBa} = 0.5m$; $b = 0.25m$	$m_{IViBa} = 0.25m$; $b = 0.5m$	$m_{IViBa} = 0$; $b = 0.75m$
k_{IViBa} (N/m)	505.06	809.38	484.6	361.6	459.4	735.18
c_{IViBa} (Ns/m)	9.38	28.12	69.6	5.04	7.89	14.98

using the SaDE algorithm was employed to identify the optimal device parameters that minimise the ground-to-structure displacement transfer function. The results demonstrated that while the TMDI configuration generally yields slightly better vibration mitigation, particularly for higher mass ratios, the TID configuration achieves comparable performance with significantly reduced internal motion of the device. This reduction in the internal motion implies lower mechanical demands and less required space for installation. Furthermore, due to the absence of the secondary mass, the required physical mass of the IViBa with a TID configuration is significantly reduced. Overall, the study confirms the effectiveness of the TID configuration as a vibrating barrier and highlights its potential as a compact, efficient, and structurally feasible alternative for real-world applications.

Acknowledgements

The first author is supported by the Marie Skłodowska-Curie Postdoctoral Fellowship under the European Union's Horizon Europe research and innovation programme (Grant Agreement No. 101153525). The second author is supported by the Project PNRR - MUR DM 118 - CUP E14D23001710006118/2023 and PRIN 2022 "BIO-RESTORE–BIO-based Resilient Energy and Seismic retrofiT Of the REsidential building stock", Prot. 202234HM8J, CUP E53C24002680006, Bando Prin 2022 – Decreto Direttoriale n. 104 del 02-02-2022. The authors gratefully acknowledges the support of these fundings.

References

Cacciola, P., Tombari, A., 2015. Vibrating barrier: a novel device for the passive control of structures under ground motion. Proceedings of the Royal Society A: Mathematical, Physical and Engineering Sciences 471(2179), 20150075.

Cacciola, P., Tombari, A., Giaralis, A., 2020. An inerter-equipped vibrating barrier for noninvasive motion control of seismically excited structures. Structural Control and Health Monitoring 27(3), e2474.

Deastra, P., Wagg, D. J., Sims, N. D., Mills, R. S., 2023. Experimental shake table validation of damping behaviour in inerter-based dampers. Bulletin of Earthquake Engineering, 21(3), 1389-1409.

Deastra, P., Dogan, H., Xie, R., Ikago, K., 2025. Shake table experimental validation of auxiliary mass effects in a tuned viscous mass damper. Structures, 80, 109681.

De Domenico, D., Deastra, P., Ricciardi, G., Sims, N. D., Wagg, D. J., 2019. Novel fluid inerter based tuned mass dampers for optimised structural control of base-isolated buildings. Journal of the Franklin Institute 356(14), 7626-7649.

Ikago, K., Saito, K., Inoue, N., 2012. Seismic control of single-degree-of-freedom structure using tuned viscous mass damper. Earthquake Engineering and Structural Dynamics, 41(3), 453-474.

Lazar, I. F., Neild, S. A., Wagg, D. J., 2014. Using an inerter-based device for structural vibration suppression. Earthquake Engineering and Structural Dynamics, 43(8), 1129-1147.

Marian, L., Giaralis, A., 2014. Optimal design of a novel tuned mass-damper–inerter (TMDI) passive vibration control configuration for stochastically support-excited structural systems. Probabilistic Engineering Mechanics, 38, 156-164.

Papageorgiou, C., Houghton, N.E.,Smith, M.C., 2009. Experimental testing and analysis of inerter devices. Journal of Dynamic Systems, Measurement, and Control 131, 011001.

Qin, A. K., and Suganthan, P. N., 2005. Self-adaptive differential evolution algorithm for numerical optimization. In 2005 IEEE congress on evolutionary computation, 2, pp. 1785-1791.

Smith, M. C., 2002. Synthesis of mechanical networks: the inerter. IEEE Transactions on automatic control, 47(10), 1648-1662.

Storn, R., and Price, K., 1997. Differential evolution–a simple and efficient heuristic for global optimization over continuous spaces. Journal of global optimization, 11(4), 341-359.

Tombari, A., Espinosa, M. G., Alexander, N. A., Cacciola, P., 2018. Vibration control of a cluster of buildings through the Vibrating Barrier. Mechanical Systems and Signal Processing, 101, 219-236.

Wagg, D. J., 2021. A review of the mechanical inerter: historical context, physical realisations and nonlinear applications. Nonlinear Dynamics, 104(1), 13-34.